

# INTERNATIONAL SOCIETY FOR SOIL MECHANICS AND GEOTECHNICAL ENGINEERING



*This paper was downloaded from the Online Library of the International Society for Soil Mechanics and Geotechnical Engineering (ISSMGE). The library is available here:*

<https://www.issmge.org/publications/online-library>

*This is an open-access database that archives thousands of papers published under the Auspices of the ISSMGE and maintained by the Innovation and Development Committee of ISSMGE.*

# Centrifuge modeling of excess pore-water pressure build-up and instability of a fill slope subject to rapid surcharge and high water level

L.T. Zhan, Z Zhang, X.G. Guo & Y.M. Chen

MOE Key Laboratory of Soft Soils and Geoenvironmental Engineering, Zhejiang University, Hangzhou, 310058, China

**ABSTRACT:** On December 20, 2015, a catastrophic landslide occurred in a 110-m-high waste dump located in Guangming New District, Shenzhen, China. This paper presents two centrifuge model tests related to this landslide. The centrifuge model was designed based on a representative section of the failed dump. It's made of construction waste from the failed dump and was composed of two units—the relatively dry and compacted front part, and the almost-saturated and loose rear part. High water level was formed in the model before centrifuge model tests. Model was tested at centrifuge accelerations of 20 g and 150 g. Pore-water pressure and displacements were measured during the tests. The results show that excess pore-water pressure was generated in the rear part due to the rapid filling. High pore-water pressure combined with reduction in suction in the soil resulted in slope failure initiated at the toe of the slope, followed by an extensive sliding.

## 1 INTRODUCTION

On December 20, 2015, a catastrophic landslide occurred in a 110-m-high waste dump located in Guangming New District, Shenzhen, China. The landslide involved  $2.51 \times 10^6 \text{ m}^3$  of construction waste, destroyed 33 buildings and killed 77 people.

The dumpsite was an abandoned quarry before receiving construction wastes beginning in February 2014. Within 22 months,  $5.83 \times 10^6 \text{ m}^3$  of construction wastes filled the dumpsite forming a 600-m-long, 400-m-wide, 110-m-high loose fill (Figure 1). The overall gradient of the slope from terraces T1 to T9 was 4H/1V (14°). The dominant component of the fill was completely decomposed granite (CDG) excavated from the adjacent underground construction. According to the investigation, the CDG at the rear part of the dump was with high initial water content. The dumping operation at the site was char-

acterized by inadequate compaction, poor water drainage and rapid filling. Inadequate compaction on the fill materials resulted in low compactness. Ineffective drainage facilities and abundant water input from surrounding area resulted in a significant rise in the phreatic surface. The rapid filling rate is likely to cause a build-up of excessive pore-water pressure in the lower poorly drained fill. The slip surface cut steeply into the very wet rear part to a maximum depth of 50 m from the ground surface, passed through the two-unit layer at a gentle inclination angle of 6° and sheared out at terrace T3 (see Figure 1).

A lot of work, mainly in numerical simulation and field investigation, have been done regarding the Shenzhen landslide (Gao et al. 2017; Liang et al. 2017; Ouyang et al. 2017; Xu et al. 2017; Yin et al. 2016; Zhan et al. 2018). However, these studies have paid little attention to physical modeling in laboratory.

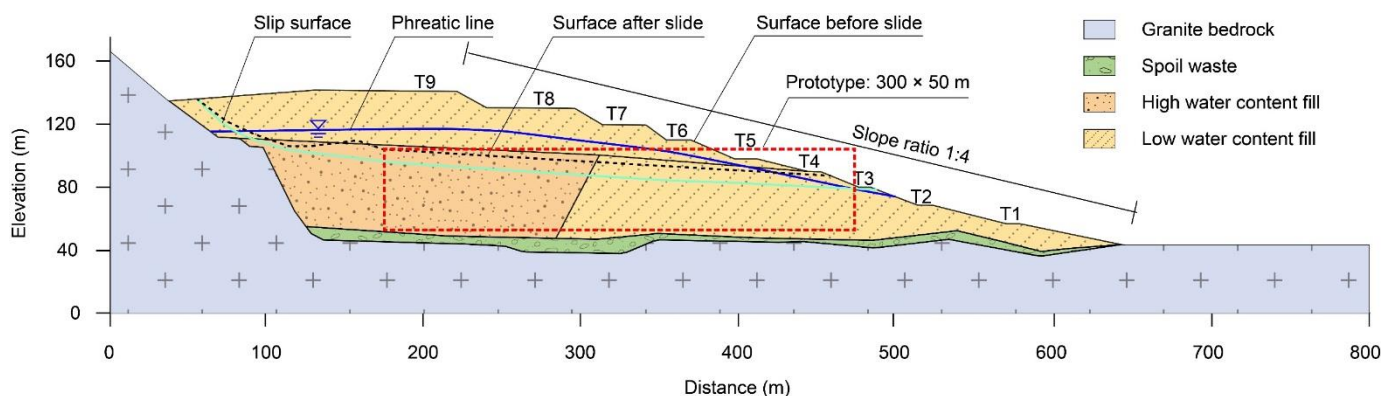


Figure 1. Geotechnical profile before and after the landslide.

Geotechnical centrifuge modeling implements high gravity to obtain similarity of stress between model and prototype. It has been widely used in scientific research and engineering practice in various fields, including the study of slope instability and deformation (Taylor 2003).

After the landslide, a project aiming at investigating the failure mechanisms and furtherly putting forward measures for disaster prevention was proposed by Zhejiang University with a financial support from NSFC. The project includes a series of centrifuge model tests and theoretical analyses with reference to this landslide. The former is intended to reproduce the failure and sliding process in laboratory. This paper presents the study of two centrifuge modeling tests, which were the pre-experiments of the project. The main objective of the centrifuge modeling tests is to understand excess pore-water pressure build-up and slope instability subject to rapid surcharge and high water level.

## 2 MODEL PREPARATION

### 2.1 Similarity relationship

Most of the geotechnical centrifuge modeling tests adopt an  $n$  g acceleration, where  $n$  is the geometrical scale, to achieve stress similarity between the models and the prototypes. The scaling laws are shown in the second column of Table 1. When very large-scale prototypes, such as high embankment and large slope, are examined, a compromise has to be made due to fixed model container size and limited centrifuge capacity. One way is to model the main part of the prototype by partial model with an equivalent stress (Liu et al. 2005). Another way is to model the prototype using a geometrical scale ( $n_l$ ) larger than the gravity scale ( $n$ ), which implies a small-scale unequal-stress centrifuge modeling. Zhang et al. (2013) models post-construction settlement of high embankment at different gravity scale with small-scale models, and fits the results to predict the full-scale results. Zhang and Hu (1991) and Iai et al. (2005) derived the scaling laws for small-scale modeling based on linear elastic assumption, as shown in the third column of Table 1.

Table 1. Similarity relationship of centrifuge test (prototype: model).

Quantity	Conventional	Small-scale
Length	$n$	$n_l$
Acceleration	$1/n$	$1/n$
Stress	1	$n_l/n$
Strain	1	$n_l/n$
Time (consolidation)	$n^2$	$n_l^2$
Displacement	$n$	$n_l^2/n$
Stiffness	1	1

However, nonlinear and elastic plastic problems dominate in practice and cannot be simply treated as linear-elastic. The scaling laws of Table 1 must be verified so that the model has a good similarity with the prototype. Zhang and Hu (1991) study the stress, strain and yield behavior of a dam, and point out that scaling laws derived under linear-elastic assumption still applies to nonlinear and elastic plastic problems if  $n_l/n \leq 2$ . Chen et al. (2011) study a slope and indicates that the equivalent plastic strain and deformation of the small-scale model are in good agreement with that of the prototype if  $n_l/n \leq 3$ .

In this experiment, part of the failed dump was modeled, as shown in Figure 1. The prototype was 300 m long and 50 m high. According to the model container size and centrifuge capacity of ZJU-400, the model was determined to be  $80 \times 40 \times 13.3$  cm (length  $\times$  width  $\times$  height) and the maximum acceleration was 150 g. The geometrical scale was 375:1 and the gravity scale was 1:150 ( $n_l = 375, n = 150, n_l = 2.5n$ ). The prototype can be deduced from the data obtained under a specific low acceleration via similarity relationship in Table 1.

### 2.2 Test setup

The centrifuge model tests were carried out with the 400 g-ton geotechnical centrifuge, ZJU-400, in Zhejiang University. A rigid aluminium container with inner dimension of  $100 \times 40 \times 100$  cm (length  $\times$  width  $\times$  height) was adopted for the model setup. The overall layout of the model is shown in Figure 2. The model was placed on a 35-cm high aluminium plate with surface rough treatment. The space below the plate was used for storing water and soil sliding out after slope failure. According to the two-unit structure of the prototype (Zhan et al. 2018), the model was made up of two parts with different initial moisture content and dry density. The front part was with a low water content of 16% and a high dry density of  $1.50 \text{ g/cm}^3$ , and the rear part was with a high moisture content of 26% and low dry density of  $1.40 \text{ g/cm}^3$ . Five piezometers, P1-P5, were placed at the bottom of the model to measure the variations of pore-water pressure. Three laser displacement transducers were placed above the model to measure the settlements of the slope. Two cameras were installed against the model section and the front slope to take photos.

### 2.3 Physical properties of model materials

The soil used in the tests was taken from the landslide site in Shenzhen and mainly composed of CDG soil. Materials of the front part of the model were taken from the surface of the post-failure dump. Materials of the rear part of the model were mixtures of borehole samples drilled from the landslide bed. According to the container size and the model size, the

maximum particle size used in the centrifuge model tests was determined to be 5 mm. According to the grain-size distribution curves, particle with diameter less than 5 mm accounted for more than 80% of the total mass, and its physical properties would resemble that of the fill materials in the dump. What's more, the maximum particle size was the same as that of the undrained compression tests and oedometer tests. The fine-grained particle (particle size less than 0.075 mm) of the materials was approximately 30-40% of the total mass.

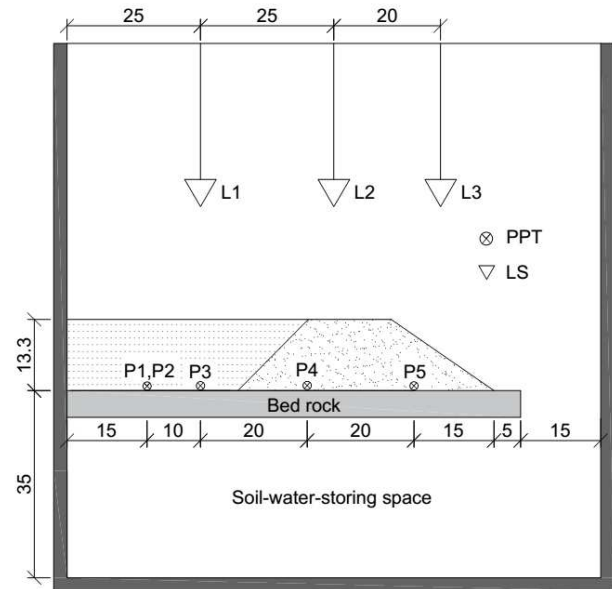


Figure 2. Test setup of the slope model (unit: cm).

According to the laboratory test, the specific gravity of the CDG soil was 2.68. The maximum dry density determined by heavy compaction test was  $1.90 \text{ g/cm}^3$  and the optimal moisture content was 12%. The plastic limit was 20.5% and the liquid limit was 39.7%, corresponding to a plasticity index of 19. The permeability coefficient was  $10^{-8}$ - $10^{-7} \text{ m/s}$  when the dry density was greater than  $1.40 \text{ g/cm}^3$ , indicating a bad permeability.

Undrained compression tests on three unsaturated specimens were performed under a constant axial strain rate of 1.25mm/min. Pore pressure and axial strain were measured every one minute during shearing. The difference of principal stress was plotted against axial strain. Yielding was thought to start at the point where difference of principal stress reached its maximum value. The principal stress and pore pressure at this point were used to calculate the effective shear strength. The test results were shown in Table 2. The effective shear strength of samples with different moisture content are close to each other.

Table 2. Shear strength of the CDG.

Moisture content	Friction angle	Cohesion
19%	28.7°	21.6 kPa
23%	24.8°	19.1 kPa
26%	27.7°	10.0 kPa

## 2.4 Model construction

The soil was passed through a 5-mm sieve to remove larger particles such as organic debris and stones. It was then oven-dried at  $110^\circ\text{C}$  for 24 hours prior to the preparation of the low and high water content soil. The soil was pulverized using a rubber hammer and spread out on a sheet of plastic. Water was added to obtain a desired moisture content (16%, 26%) and the soil was thoroughly mixed. When all soil was ready, the mixed soil was kept in a plastic box for moisture equalization for about 24 hours.

As the model was made up of two parts, we firstly constructed the front part. In constructing the front part, the slope geometry was first traced onto the inner walls of the box. Wooden plates were placed in aluminium box as support. The front part was divided into 5 horizontal layers (3, 6, 9, 12, 13.3 cm) for fill. The required amount of soil for each layer was dumped into the container and compacted to the desired height to reach the corresponding dry density. In order to make the deformation more observable, white markers with a horizontal spacing of 5 cm were set at the height of 3, 6, 9, 12 cm in the front part. After the slope attained its full height, the wooden plates were removed, and the front part was cut to the desired shape. Lastly, water was added to the rear reservoir to a height of 13 cm to form a high-water level in the front slope. After 48 hours, water in the reservoir was drained. High water content soil was dumped into the rear part and compacted in 5 horizontal layers. The finished slope (Figure 3) was covered by plastic sheets before centrifuge modeling test.



Figure 3. Side view of the model.

## 3 TEST PROCEDURES

In order to observe the build-up of pore-water pressure, especially that in the high water content rear part, and the slope instability of the front part, the centrifuge model was tested twice under different accelerations: (1) in the first test, the model was directly accelerated to 20 g and kept constant for about 40 minutes, where the model represented a 2.6-m

high prototype. The objective was to observe the instability of front slope subject to high water level; (2) in the second test, the model was accelerated to the max acceleration of 150g as quickly as possible (within 15 minutes), where the model represented a 20-m high prototype. This test aimed at understanding the build-up of excess pore-water pressure in fill slope subject to rapid surcharge. Pore-water pressures, settlements and photos were recorded during the two tests.

## 4 TEST RESULTS AND ANALYSIS

### 4.1 Failure process

Figure 4 shows the failure process of the front slope during the first centrifuge spinning. The model was stable before the acceleration attaining 18 g (Figure 4a). The laser displacement transducers above the slope showed that the surface settlement continue to develop with the increase of acceleration. When the slope was accelerated to approximately 18 g, cracks occurred at the foot of the slope and water can be observed in the cracks (Figure 4b). The water level at the slope surface was about 6 cm high. With the increase of the acceleration, the failure extended upward to the top of the slope and lots of soil slid out (Figure 4c). Eventually the failure stopped several minutes later after the acceleration attained 20 g and kept constant.

### 4.2 Pore-water pressure of the first test

Figure 5 shows the response of the pore-water pressure of the first test recorded from the start of centrifuge spinning. The pore-water pressure increased with the acceleration. After attaining the targeted acceleration of 20g, the pore-water pressure started to dissipate.

The reading of P1 fluctuated with time after attaining 20 g and then kept unchanged, which was 35 kPa. The fluctuation might be related to the unsaturation of the rear part ( $w = 26\%$ ,  $S_r = 77\%$ ).

The readings of P2 and P3, which were located at the rear part, were nearly the same during the test. The maximum readings were 44 kPa and 45 kPa, respectively. As the model was 13.3 cm high, the hydrostatic pressure was 27 kPa at most ( $0.133 \times 20 \times 10 = 27$  kPa), corresponding to excess pore-water pressure of 17 kPa and 18 kPa at least. It's worth noting that the pore-water pressure did not show significant change at the instant of failure. Pore-water pressure of P2 and P3 dissipated slowly after attaining 20 g due to long distance from the front slope and low permeability.

The readings of P4 and P5, which were located in the front part, were close to each other and much lower than that of P1, P2 and P3. The maximum pore-water pressure was 18 kPa and 16 kPa, respectively, corresponding to water level of about 9 cm

and 8 cm if no excess pore-water pressure existed in P4, P5. This is consistent with the observed water level in the cracks. Pore-water pressure did not show significant change at the instant of failure but decreased quickly after attaining to 20 g due to the sliding out of water and soil.

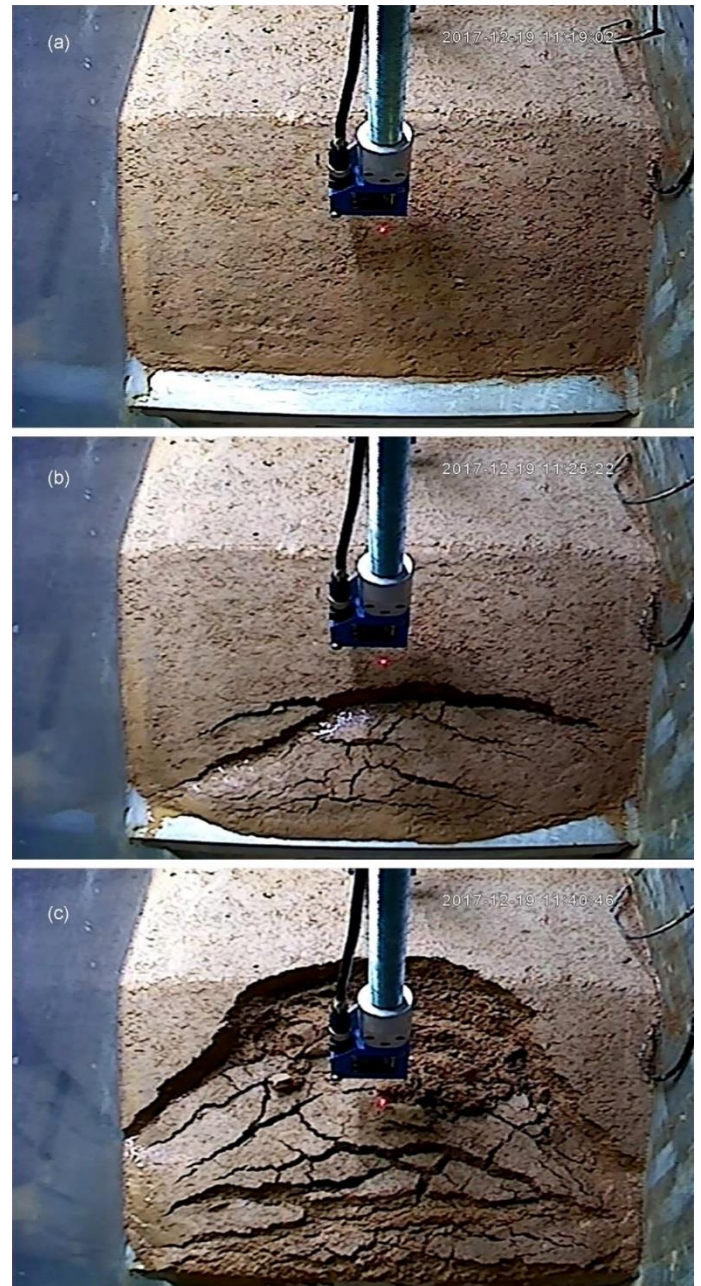


Figure 4. Failure of model slope: (a) 0 g; (b) 18 g; (c) 20 g.

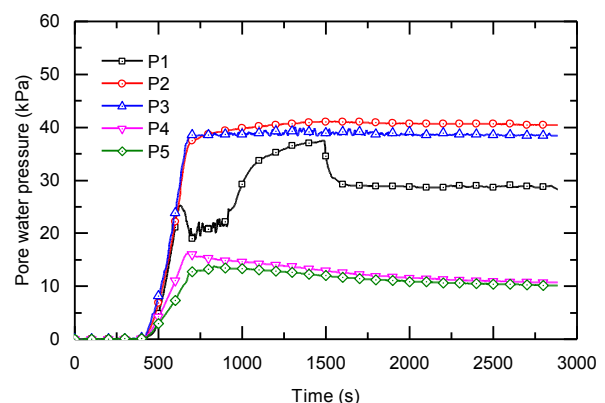


Figure 5. Variations of pore-water pressure.

### 4.3 Back analysis

Back calculations were performed by using SLOPE/W with Morgenstern-Price limit equilibrium analysis based on the modified Coulomb failure criteria (Equation 1), which is applicable to partially saturated soil (Ling and Ling 2012).

$$\tau = c' + (\sigma - u_a) \tan \phi' + (u_a - u_w) \tan \phi^b \quad (1)$$

where  $c'$  = effective cohesion;  $\phi'$  = effective friction angle associated with net stress ( $\sigma - u_a$ );  $\phi^b$  = friction angle associated with a change in suction ( $u_a - u_w$ );  $c' + (u_a - u_w) \tan \phi^b$  = apparent cohesion.

The ground water level in the model slope was determined based on the measured pore-water pressure data from the P1, P2, P3, P4 and P5 (Figure 6). It's assumed that pore-water pressure readings at P4 and P5 was composed solely of hydrostatic pressure, which corresponding to a water level of 9 cm and 8 cm. The water level at the rear part was assumed to be 13.3 cm for its high water content. The maximum suction for the rear and front part materials was 10 kPa and 100 kPa according to soil water characteristic curves of CDG samples.

The back analyses set the factor of safety (FoS) to unity to back-calculate the strength. The variation in the angle of friction with moisture was rather small and was considered a constant ( $\phi' = 28^\circ$  according to Table 2). The back calculations showed that a similar failure mode (Figure 6) would occurred when the  $c'$  was 2 kPa and  $\phi^b$  was  $17^\circ$  (about half of  $\phi'$ ). When the water level in the front part was lower, the FoS would be greater than one, indicating a stable state. For example, the FoS was about 1.25 when pore-water pressure at P4, P5 was set to zero even if without taking the suction into account ( $\phi' = 28^\circ$ ,  $c' = 2$  kPa,  $\phi^b = 0^\circ$ ). If the suction was taken into account, the FoS was about 4.68, indicating a more stable state.

The back calculations show that the high water level, which decreases the effective stress as well as the suction in the soil, can significantly reduce the stability of the slope.

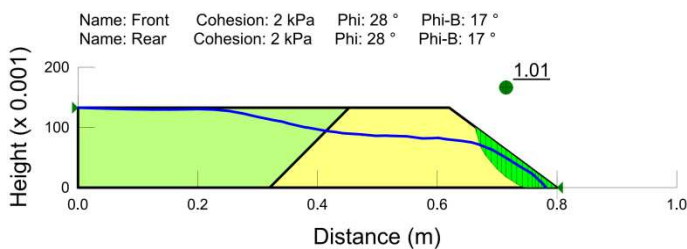


Figure 6. Back calculations by using 2-D numerical model with LEM.

### 4.4 Pore-water pressure of the second test

The second test was to investigate the build-up of excess pore-water pressure in high water content fill

subject to rapid surcharge (modeled by accelerating the model from 0 g to 150 g within 15 minutes). Figure 7 presents the time histories of the pore-water pressure during the second test. The pore-water pressure increased with the acceleration and started to dissipate after attaining the targeted acceleration of 150g.

The readings of the three transducers P1, P2 and P3, which were located at the rear part, were nearly the same during the test. Their maximum readings were 275 kPa, 275 kPa and 245 kPa, respectively. As the hydrostatic pressure was 200 kPa at most ( $150 \times 0.133 \times 10 = 200$  kPa), the excess pore-water pressure was 75 kPa, 75 kPa and 45 kPa at least.

The readings of the two transducers P4, P5 in the front part were much lower than that of P1, P2 and P3. The maximum pore-water pressure was 150 kPa and 75 kPa, respectively. It's worth noting that P4 and P5 recorded significant change when the model was subject to 50 g, where a large-scale failure occurred.

Take the 1-cm thick soil at the bottom of the model for analysis, pore-water pressure, hydrostatic pore-water pressure and excess pore-water pressure was determined according to transducers P1-P5. Effective overburden stress was obtained according to the total overburden pressure, which could be determined according to the dry density, water content and acceleration. The ratio of excess pore-water pressure to effective overburden stress (pore-water pressure ratio) was calculated. Its value was about 0.50 when the acceleration was 150 g.

This value can be used to estimate the excess pore-water pressure caused by the rapid loading of the fill at the dump: (1) the complete prototype corresponds to an unequal stress model ( $n_i/n = 2.5$ ) with a total height of 24 cm and a water level of 14 cm at the rear part. The maximum overburden effective stress of the 1-cm thick soil at the bottom is about 392 kPa; (2) the surcharge-induced excess pore-water pressure at the model is estimated to be  $392 \times 0.5 = 195$  kPa; (3) the excess pore-water pressure at the prototype is  $196 \times 2.5 = 490$  kPa according to the scaling laws in Table 1. The prediction is close to the result calculated according to the numerical simulation on the real case.

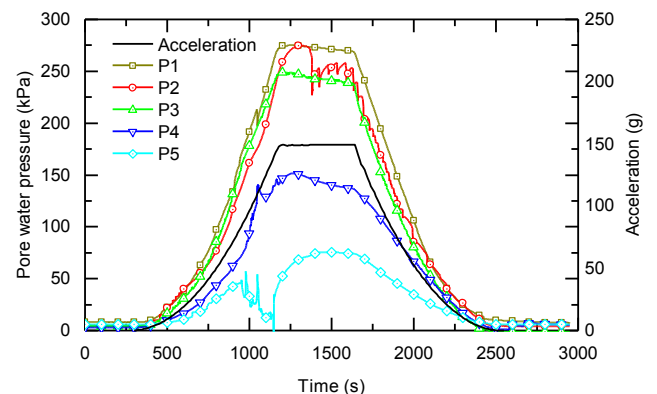


Figure 7. Variations of pore-water pressure.

## 5 CONCLUSIONS

This paper presents two centrifuge model tests of a fill slope subject to rapid surcharge and high water level. The following conclusions are drawn from the study:

1. The failure observed in the first test initiated at the base of the slope, extended upward and finished with an extensive landslide.
2. A high pore-water pressure combined with a reduction in suction due to high water level in the soil were responsible for the slope failure.
3. Excess pore-water pressure up to 18 kPa and 75 kPa was generated in the high water content rear part during two tests. The ratio of excess pore-water pressure to effective stress was about 0.5 under an acceleration of 150 g, and it could be used to estimate the excess pore-water pressure in the prototype.

The use of equal-stress centrifuge modeling, numerical and theoretical analyses were suggested for further studies. Comparing with this paper may gain more understanding.

## 6 ACKNOWLEDGEMENTS

The research of this paper was sponsored by National Natural Science Foundation of China (NSFC Grant no. 41641028, 51625805).

## 7 REFERENCES

- Chen, X.P., Huang, J.W., Ng, C.W.W. & Ma, S.K. 2011. Centrifugal model tests on ancient bank landslide. *Yantu Gongcheng Xuebao/Chinese Journal of Geotechnical Engineering* 33(10): 1496-1503.
- Gao, Y., Yin, Y.P., Li, B., Wang, W.P., Zhang, N., Yang, C.X. & Zuo, X. 2017. Investigation and dynamic analysis of the long runout catastrophic landslide at the Shenzhen landfill on December 20, 2015, in Guangdong, China. *Environmental Earth Sciences* 76(1): 13.
- Iai, S., Tobita, T. & Nakahara, T. 2005. Generalised scaling relations for dynamic centrifuge tests. *Geotechnique* 55(5): 355-362.
- Liang, H., He, S.M., Lei, X.Q., Bi, Y.Z., Liu, W. & Ouyang, C.J. 2017. Dynamic process simulation of construction solid waste (CSW) landfill landslide based on SPH considering dilatancy effects. *Bulletin of Engineering Geology and the Environment*:1-15.
- Ling, H. & Ling, H.I. 2012. Centrifuge model simulations of rainfall-induced slope instability. *Journal of Geotechnical and Geoenvironmental Engineering* 138(9): 1151-1157.
- Liu, H., Zhang, Z.Y. & Han, W.X. 2005. Centrifugal model technique of high embankment. *Geological Science and Technology Information* 24(1): 103-106.
- Ouyang, C.J., Zhou, K.Q., Xu, Q., Yin, J.H., Peng, D.L., Wang, D.P. & Li, W.L. 2017. Dynamic analysis and numerical modeling of the 2015 catastrophic landslide of the construction waste landfill at Guangming, Shenzhen, China. *Landslides* 14(2): 705-718.
- Taylor, R.E. ed. 2003. *Geotechnical centrifuge technology*. CRC Press.
- Xu, Q., Peng, D.L., Li, W.L., Dong, X.J., Hu, W., Tang, M.G. & Liu, F.Z. 2017. The catastrophic landfill flowslide at Hongao dumpsite on 20 December 2015 in Shenzhen, China. *Natural Hazards and Earth System Sciences* 17(2): 277.
- Yin, Y.P., Li, B., Wang, W.P., Zhan, L.T., Xue, Q., Gao, Y., Zhang, N., Chen, H.Q., Liu, T.K. & Li, A.G. 2016. Mechanism of the December 2015 catastrophic landslide at the Shenzhen landfill and controlling geotechnical risks of urbanization. *Engineering* 2(2): 230-249.
- Zhan, L.T., Zhang, Z., Chen, Y.M., Chen, R., Zhang, S., Liu, J. & Li, A.G. 2018. The 2015 Shenzhen catastrophic landslide in a construction waste dump: Reconstitution of dump structure and failure mechanisms via geotechnical investigations. *Engineering Geology* 238: 15-26.
- Zhang, J.H., Huang, X.N., Zheng, J.L., Wei, J.M. & Xu, X.J. 2013. Centrifugal model tests on post-construction settlement of high embankment of Hechi Airport. *Chinese Journal of Geotechnical Engineering* 35(4): 773-778.
- Zhang, L.M. & Hu, D. 1991. Numerical evaluation of the similitudes for large-scaled centrifuge models. *In Proceedings of International Symposium on Landslide and Geotechnics*: 65-69.